Ceramics International **24** (1998) 347–357

PII: S0272-8842(97)00021-7
0272-8842/98 $19.00+.00

Drying Kinetics of Water-Based Ceramic Suspensions for Tape Casting

B. J. Briscoe,* G. Lo Biundo & N. Özkan

Particle Technology Group, Department of Chemical Engineering and Chemical Technology, Imperial College, London, UK

(Received 25 October 1996; accepted 10 January 1997)

Abstract: An experimental study is described which seeks to characterise the drying kinetics of water-based ceramic (alumina) suspensions in controlled environments. The drying process of the ceramic suspensions is shown, to a first approximation, to follow a two stage mechanism (initial stage: 'external' evaporation controlled process; and second stage: 'internal' diffusion-controlled process). It has been shown that the temperature, the humidity and the surface area of the samples strongly affects the drying kinetics of these suspensions in the initial stage of the drying. The thickness of the samples is more influential in the second stage of the drying. There are no noticeable effects of the initial solid content and the nature of binder content of the suspensions on the drying kinetics. A first order empirical relationship is provided in order to predict the drying time and drying curve for these ceramic suspensions. The drying curves of tape cast suspensions is shown to be predicted accurately by the use of this relationship.

1 INTRODUCTION

Tape casting is a well established technique for the large-scale manufacturing of thin and flat ceramic products.[1–4] The typical applications for these tape cast products are substrates (Al_2O_3, AlN) for thin film circuitry, capacitors ($BaTiO_3$), solid electrolytes ($Ce_{0.9}Gd_{0.1}O_{1.95}$, YSZ) for sensors and solid oxide fuel cells, piezoelectric ceramics for actuators and transducers, SiC for heat exchangers, and MgO based materials for photovoltaic solar energy cells. Organic solvents[3] (alcohols, ketones, hydrocarbons) are frequently used to prepare the required concentrated ceramic suspensions with the necessary reproducible rheological and drying behaviours. The drying process of ceramic suspensions is one of the most important unit operations which plays a significant role in the economy of the whole manufacturing process. Due to the volatility and toxicity of these organic solvents, the development of water-based tape casting systems is considered to be desirable. The water-based suspension systems have the advantages of non-flammability, non-toxicity, and low cost. In addition, there is also an extensive knowledge base available for the processing water-based systems which are used for other ceramic processing techniques. However, the water-based suspensions have a smaller tolerance to minor changes in the drying conditions, casting compositions or film thicknesses and also the drying rate of the water-based suspensions is invariably much slower than that of the non-aqueous systems. Crack-free, uniform green tapes may only be produced using properly optimised water-based suspensions under well controlled conditions.

Even though many publications concerning the use of water-based suspension formulations for tape casting have been reported recently in the literature,[5–8] there is little reported recently on the drying kinetics of the water-based or indeed organic solvent based, suspensions. The basic principles of the 'air-drying' of such materials was however clearly expounded almost 70 years ago by Sherwood in a series of papers.[9] The early papers laid down the foundation of the current appreciation of the various stages of the drying processes of suspensions. In this study, the drying kinetics,

*To whom correspondence should be addressed.

based mainly on gravimetric data, of certain water-based alumina suspensions are reported. The effects of the ambient temperature and humidity, the surface area and the thickness of the alumina tapes, and the flow rate of the gas (water vapour and nitrogen mixture) on the drying kinetics of the suspensions are investigated experimentally. A first-order empirically based relationship is developed in order to predict the drying behaviour for the current tape cast alumina suspensions. The basic finding are consistent with the conclusions drawn by Sherwood[9] but in addition provides a more quantitative characterisation of the behaviour of these systems.

2 EXPERIMENTAL PROCEDURE AND MATERIALS

2.1 Equipment for weigh loss recording

In order to record the weight loss as a function of time, two types of micro balance systems (Cahn D-200 and Sartorius MC1) were used. The Cahn D-200 micro balance has a relatively low mass capacity of 5 g and a high sensitivity of 0.001 mg. This system may be used in different environments such as low vacuum, flowing gases or atmospherically controlled conditions. The ambient temperature and humidity may also be controlled accurately in this system. A schematic representation of this system is illustrated in Fig. 1. In order to record the weight loss of those tape cast suspensions with larger surface areas, the Sartorius MC1 micro balance system, which has a capacity of 200 g and a sensitivity of 0.01 mg was used. This system has no rigorous environmental control. A schematic representation of the Sartorius MC1 micro balance system is shown in Fig. 2.

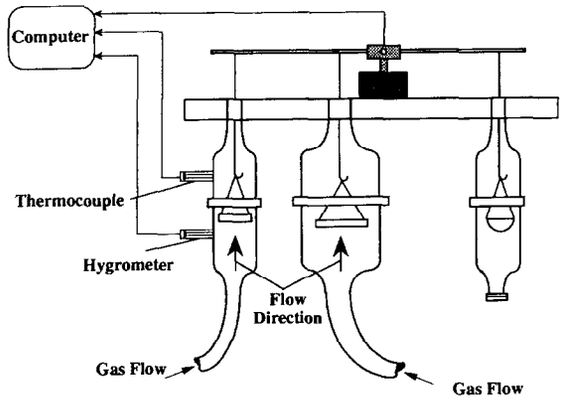

Fig. 1. The schematic representation of the Cahn D-200 micro balance system.

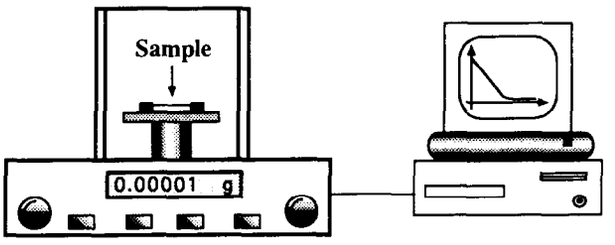

Fig. 2. The schematic representation of the Sartorius MC1 micro balance system.

2.2 Materials

The powder used in this study was a commercially available alumina (Alcoa A16 SG U.K.) with an average particle size of 0.5 μm and a surface area of *ca.* 9.8 m^2 g^{-1}. 'Duramax D-3021' (Rohm and Hass, USA) and 'Duramax B-1035' (Rohm and Hass, USA) were used as the dispersant and the binder, respectively; these materials are commonly used in the formulation of alumina suspensions and greens in commercial tape casting processes.

2.3 Tape casting

The general preparation procedure for the production ceramics foils using the tape casting method for water-based suspensions is outlined in Fig. 3; in the present paper the only stages up to that of the drying stage are considered. First, the alumina powder, the dispersant, and water were mixed using a ball milling technique at *ca.* 25°C. Zirconia balls, 200 g, with a diameter of *ca.* 5 mm were used as a milling media housed in a rotary horizontal cylinder of diameter and length 0.07 and 0.13 m, respectively. The rotational velocity was 70 rpm. Typically, the volume of the charge of water and alumina was *ca.* 20% of the volume of the cylinder. As recommended by the manufacturers (Rohm and Hass), upon the introduction of the binder, the suspension was ball milled slowly (10 rpm) for *ca.* 15 min. In order to eliminate the air bubbles, which are formed during the ball millings, the suspension was stored under low vacuum until all the bubbles were destroyed (*ca.* 10–15 min). The tape casting operation was carried out using the appropriate sample holders for the micro balance systems. Two types of sample holders were used in this study (Fig. 4). For the Cahn D-200 micro balance system, a cylindrical 'Pyrex' glass container (diameter = 26 mm and height = 3 mm) was used. Square sample holders with various surface areas up to 50 cm^2 were used for the Sartorius MC1 micro balance system. After casting the suspension on to the appropriate container, the weight loss of the samples, as a function time, was recorded using the micro balance systems. The formulations of the

alumina suspensions used in this study are given in Table 1; for convenience, the final suspensions have been coded for subsequent reference purposes.

3 RESULTS AND DISCUSSION

Experiments have been performed in order to obtain a first order description of the drying kinetics which contain the important parameters such as the thickness and the surface area of the tapes, the suspension properties (solid content and binder content), the temperature, the relative humidity, and the ambient gas flow rate.

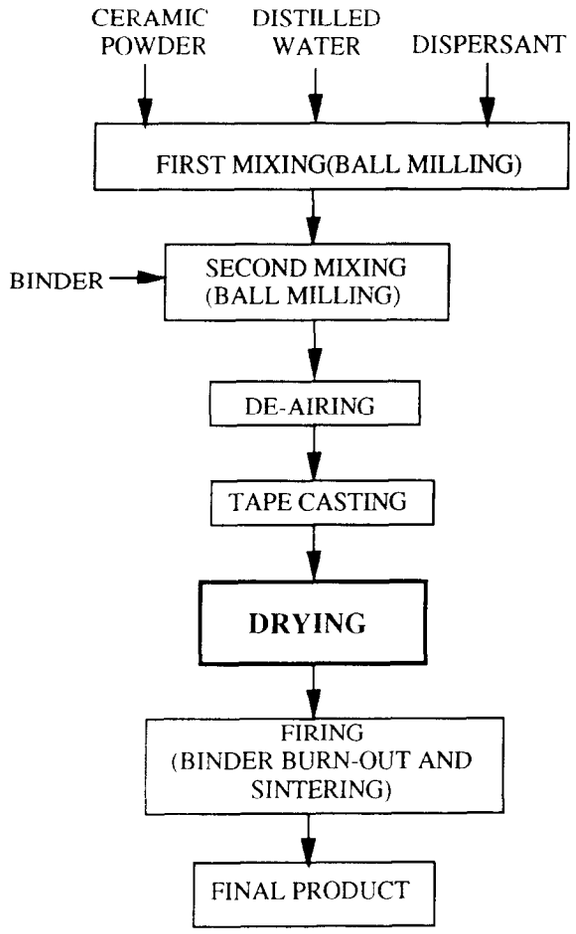

Fig. 3. The preparation procedure for the tape casting of the alumina suspensions.

3.1 Effects of temperature on drying process

When liquid water is in contact with its vapour phase, the boundary between the two homogeneous phases is not simply a mathematical plane. This interface region may be thought as a very thin film (interfacial phase) whose properties are different from the two adjacent phases. The rate of evaporation of liquid water, from a such surface phase, can be well expressed by the following equation:[10]

$$\frac{dW}{dt} = K\exp\left(-\frac{E}{RT}\right) \quad (1)$$

where dW/dt (kg s^{-1}) is the rate of weight loss for the water during the evaporation process, K (kg s^{-1}) is a constant, E (kJ mol^{-1}) is the activation energy for the evaporation, R (kJ mol K^{-1}) is the gas constant, T (K) the absolute temperature, and t (s) is the time. The parameters K and E are characteristics of this interface phase which will also have a temperature somewhat lower than the ambient due to the latent heat of evaporation.

In order to estimate the activation energy, E, for the water evaporation, the weight loss of the water phase alone, at various temperatures into an effective infinite vapour sink of relative humidity 40%, was recorded as a function time. The weight loss curves for the water at 25, 40, and 55°C are illustrated in Fig. 5. After calculating the evaporation rate from the weight loss curves, the activation

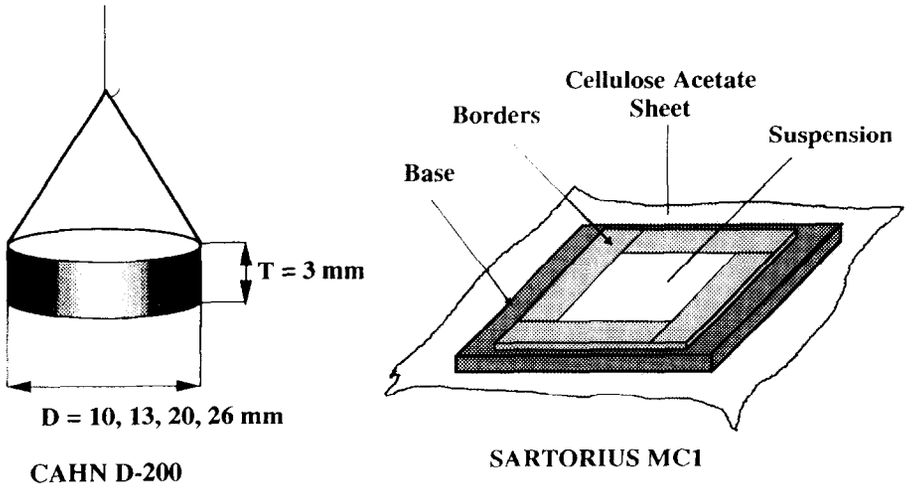

Fig. 4. The sample holders for the tape casting of the alumina suspensions.

Table 1. The formulations of the alumina suspensions used in this study

Suspension	Solid (Al_2O_3) content (vol%)*	Binder content (wt%)†	Dispersant (wt%)‡
1	40	13	0.75
2	42	13	0.75
3	44	10	0.75
4	40	6	0.75
5	39	14	0.75

*Initial solid content = the volume of the alumina powder / the total volume of the suspension.
†Initial binder content = the weight of the binder / the weight of the powder.
‡Initial dispersant content = the weight of the dispersant / the weight of the powder.

energy for the water evaporation was estimated as 42 ± 2 kJ mol^{-1} from the slope of the plot of ln (dW/dt) against ($1/T$) (see Fig. 6). The estimated activation energy for the water evaporation agrees well with the value of 44 kJ mol^{-1}, given in the literature[10] for pure water. The accepted value for the enthalpy of evaporation of water, which is temperature dependent, is about 43.5 kJ mol^{-1} in this temperature range.[11] Similarly, the activation energies for the evaporation process of the water-binder mixtures and the alumina suspensions (Table 1) were also estimated. The weight loss curves and the Arrhenious plot for an alumina suspension (suspension-5) are illustrated in Figs 7 and 8, respectively. The activation energy results for these systems are summarised in Table 2 for various temperatures and relative humidity values; all the activation energy values are of very similar magnitudes. As may be seen from Fig. 7, the large portion of the drying curves follow a linear relationship during the drying process. Therefore, it

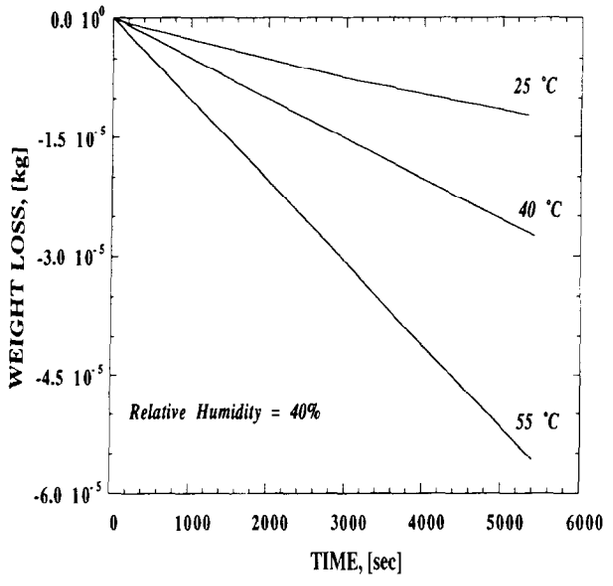

Fig. 5. The weight loss curves of the water at 25, 40 and 55°C.

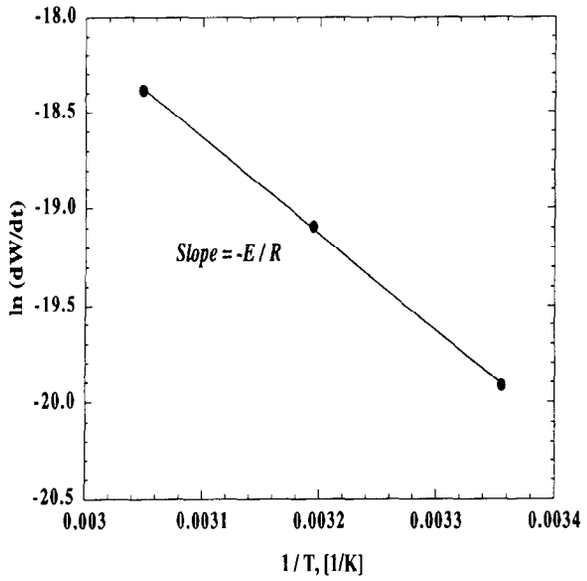

Fig. 6. The Arrhenius plot (ln (dW/dt) against $1/T$) for the evaporation process of the water.

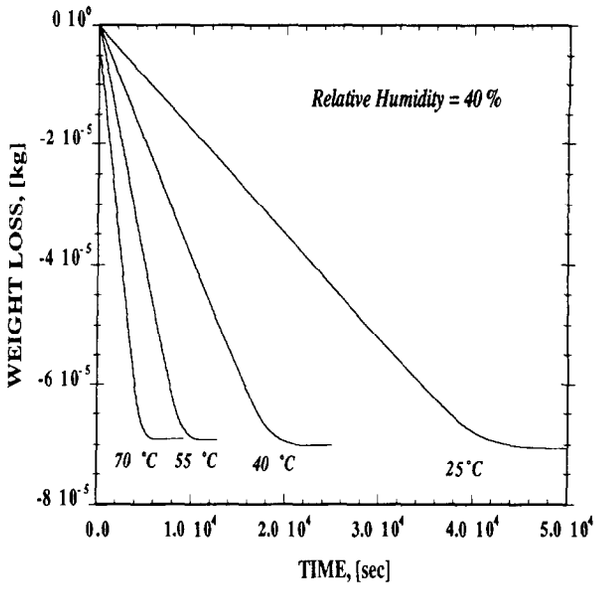

Fig. 7. The drying curves of the alumina suspensions at 25, 40, 55 and 70°C and the relative humidity of 40%.

may be concluded that the drying process of the suspensions is controlled by the evaporation process from the interface phase until the drying curve deviates from the straight line. What is more, it would appear that in this region the system behaves as though it is composed only of water and the particulates and organic additives have no major influence upon the drying process. During the initial stage, which is controlled by the evaporation process, the resistance for the transport of water to the surface of the sample is apparently negligible compared with the resistance at the liquid/vapour interface. This regime was identified by Sherwood[9] as a general characteristic of a 'very wet' solid. The point after which the drying curve deviates from the straight line, the 'falling rate

Table 2. The values of the rate of drying and the activation energies for different systems

System	Humidity (%)	dW/dt(kg s^{-1})* 298±2 K	313±2 K	328±2 K	E (kJ mole^{-1})
Water	40±2	−2.2 e-9	−5.1 e-9	−1.0 e-8	41.4±2
Water-Binder	40±2	−2.2 e-9	−5.1 e-9	−1.0 e-8	41.8±2
Suspension-5	40±1	−1.7 e-9	−3.8 e-9	−7.9 e-9	40.6±2
Suspension-5	65±3	−1.0 e-9	−2.0 e-9	−4.7 e-9	40.9±2
Suspension-5	90±2	−3.2 e-10	−4.5 e-10	−15.4 e-10	42.1±2

*All these values are calculated with an error of about ±0.1 e-9 kg s^{-1}.

period',[9] is subsequently referred to as the 'critical point'. After this critical point, the drying process is now controlled by the transportation of the water to the surface of the sample (diffusion process). The overall contribution of the diffusion-controlled process during the drying of the suspensions is quite small and as the thickness of the samples is reduced this contribution becomes even smaller in terms of the necessary total drying time.

In summary, in the initial stage of the drying process, the rate of drying is constant until the critical point suggesting that the solid and organic content of the suspension does not greatly affect the rate of drying since the solid (particulate and organic components) content of the system increases as the drying process continues. In order to further confirm the aforementioned point, the weight loss curves for suspensions with various initial solid contents were obtained and it has been observed that the weight loss curves of these suspensions were nearly identical. After the critical point the process is now controlled, in part, by the particulates as they influence the mobility of the water within the solid structure.

3.2 Effects of humidity on drying process

In order to establish the effects of the relative humidity on the drying kinetics of the alumina suspensions, the drying curves for the relative ambient humidities of 40, 65, and 90% were recorded continuously. Figure 9 shows the drying curves of an alumina suspension for the relative ambient humidities of 40, 65, and 90% at the room temperature, 25°C. As may be seen from Fig. 9, the rate of drying is strongly affected by the relative humidity; that is, the rate of drying is reduced with the increasing of the relative humidity.

The drying rates of the suspensions for the various relative humidity levels are summarised in Table 3. The influence of the relative humidity will be subsequently incorporated into eqn (1) through the constant, K, introduced in Section 3.5.

3.3 Effect of the initial tape thickness on drying kinetics

In order to establish the general effects of the thickness of the samples on the drying kinetics, the weight loss of samples, with various final thicknesses (0.6, 0.9, and 1.25 mm), was recorded during

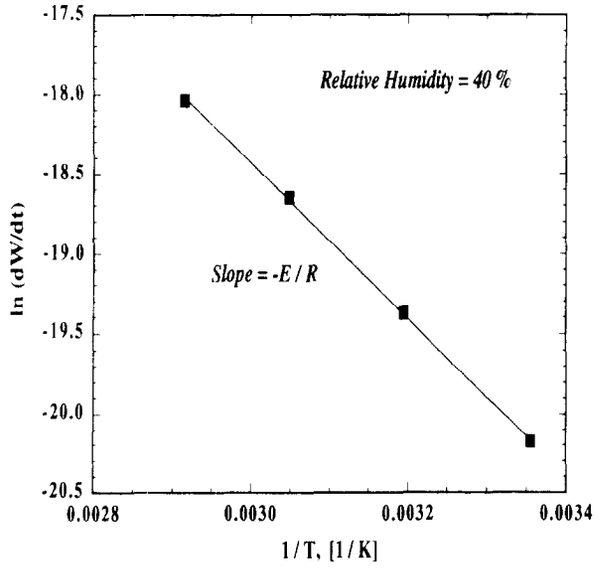

Fig. 8. The Arrhenius plot (ln (dW/dt) against $1/T$) for the evaporation process of the alumina suspensions.

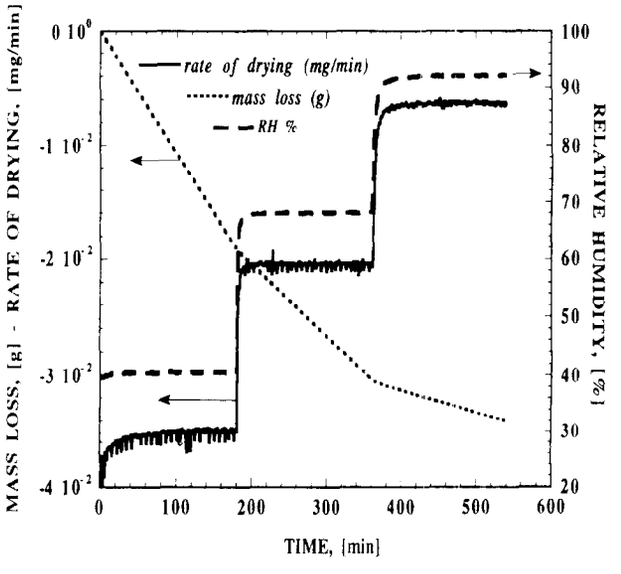

Fig. 9. The mass loss and drying rate curves for the alumina suspension at various humidity levels.

Table 3. *K* values for the suspension-5 (see Table 2)

Relative humidity (%)	K(kg s^{-1})		
	298 K	313 K	328 K
40	−0.02968	−0.03015	−0.03015
65	−0.01725	−0.01516	−0.01716
90	−5.38e-3	−3.422e-3	−5.65 e-3

the drying process. The drying curves for these samples are illustrated in Fig. 10. As may be seen from Fig. 10, the thickness of the samples does not detectably affect the drying kinetics of the suspensions during the initial stage of the drying. This behaviour is in accord with the fact that the drying of the suspension in the initial stage is controlled by the interfacial phase evaporation process. It may also be noticed that the contribution of the subsequent diffusion-controlled process becomes more pronounced as the thickness of the samples increases. The normalised weight loss curves, as a function of the lapsed time, for the suspensions with various thicknesses are illustrated in Fig. 11. This observation further confirms that the drying of the suspensions is initially controlled by the surface evaporation process until the so-called 'critical point' and after this point the internal diffusion mechanism becomes the controlling mechanism for the drying of these ceramic suspensions.

The water content at the critical point was calculated as *ca.* 10.0 wt% (relative to the initial total water content in the suspension with the 39.0 vol% solid content). Therefore, it can be concluded that only *ca.* 10 wt% of the water in the suspension is lost during the diffusion-controlled stage and that the larger portion of the water in the suspension

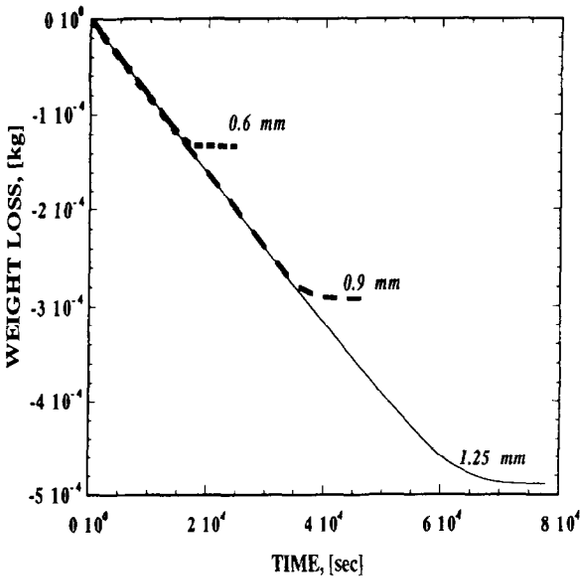

Fig. 10. The drying curves of the alumina suspension with the thicknesses of *ca.* 0.6, 0.9 and 1.25 mm.

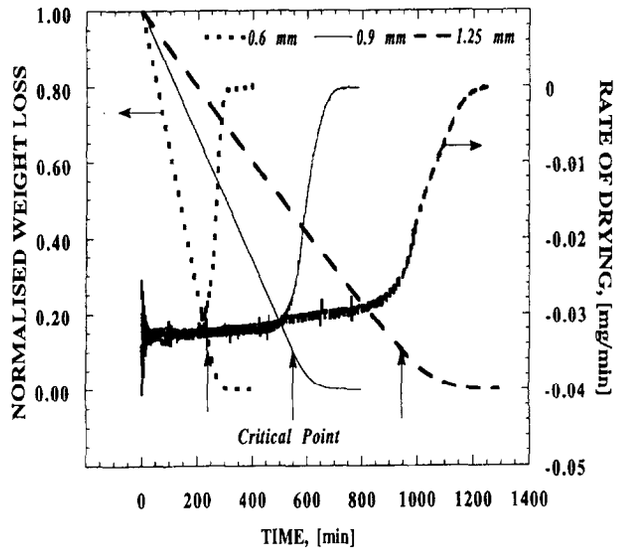

Fig. 11. The normalised drying curves of the alumina suspension with the thicknesses of *ca.* 0.6, 0.9 and 1.25 mm.

(*ca.* 90 wt%) is lost during the first stage (evaporation). At the critical point the vol% of water, air, organic additives, and alumina powder was *ca.* 5.92, 16.46, 18.22, and 59.40, respectively. An analytical solution which may be used to describe to the second stage of the suspension drying process will be reported in Section 3.5.

3.4 Effects of surface area of samples on drying kinetics

In order to investigate the effects of the sample exposed surface area on the drying kinetics of the suspensions, the MC1 micro balance was used since the D-200 micro balance was not suitable for the study of larger samples (the maximum sample size for this system is limited to 3 mm in diameter). It is also difficult to determine the effective surface area of the suspensions in the small sample holders due to the concave shape of the liquid surface in these containers. The drying curves of the suspensions with various exposed surface areas are illustrated in Fig. 12. A linear interrelationship between the drying rate and the surface area is observed; this is consistent with the simple expectation that the drying rate will scale in a linear way with the exposed surface area.

3.5 Effects of flow rate on the drying kinetics

In order to establish, in a preliminary way, the effects of the ambient gas flow rate on the drying kinetics of the alumina suspensions, the drying curves of the alumina suspensions at various ambient gas flow rates were obtained. As can be seen from Fig. 13, the drying rate of the alumina suspensions increases with the increasing of the

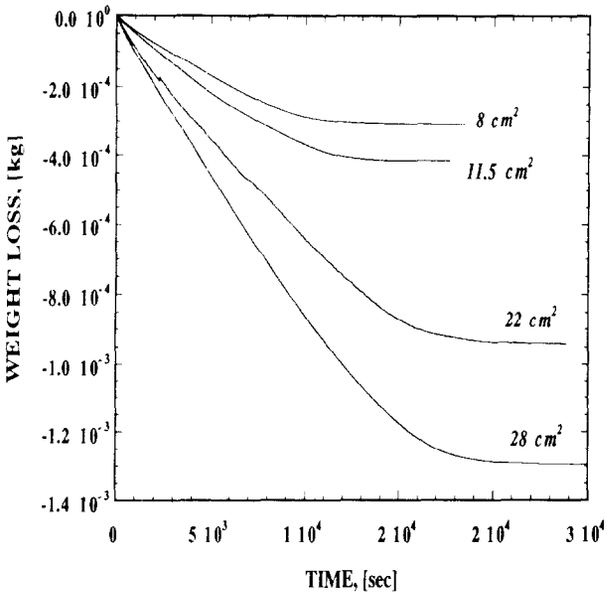

Fig. 12. The drying curves of the alumina suspensions with various surface areas.

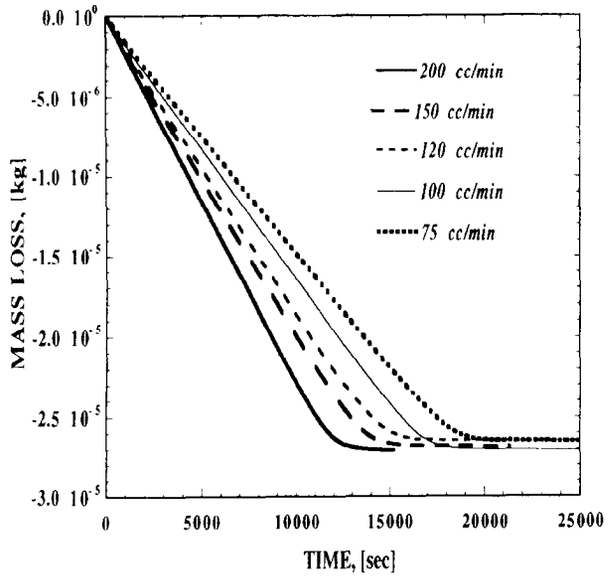

Fig. 13. The drying curves of the alumina suspensions with various flow rates.

flow rate. This observation indicates that the flow rate influences the properties of the interface region, a so-called 'stagnant layer', between the ambient vapour and the interfacial liquid phase of the suspension and that the evaporation from this interface region becomes more effective with the increasing of the ambient gas flow rate. The influence of this important variable is not examined further in the present paper and will be considered in a future publication.

3.6 A first order empirical model for suspension drying

In the previous sections, it has been shown that the drying kinetics of the alumina suspensions is affected by the temperature, the relative humidity, and the surface area of the sample during the initial stage of drying and by the thickness of the sample during the second stage of drying. The ambient gas flow rate also influences the drying rate. Therefore, a sufficient general drying rate equation, excluding the influence of the ambient gas flow rate, for these ceramic suspensions, in the initial stage of the drying, should contain these aforementioned parameters and may be written in the following form:

$$\frac{dW}{dt} = AK\exp\left(-\frac{E}{RT}\right) \tag{2}$$

where dW/dt is the drying rate (kg s^{-1}), A (m^2) is the surface area of the sample, K (kg m^2 s^{-1}) is a constant which depends upon the relative humidity, E is the activation energy for the evaporation process, R is the gas constant, T is the absolute temperature. In order to establish the dependence of K upon the relative humidity, the drying rates of suspensions at constant temperature are plotted against the relative humidity. Figure 14 shows a plot of the constant, K, against the ambient relative humidity. As may be seen from Fig. 14, there is a linear interrelationship between K and the ambient relative humidity; this is to be expected if the interface phase is simply behaving as though it were water. Then, eqn (2) becomes:

$$\frac{dW}{dt} = A(a + bH)\exp\left(-\frac{E}{RT}\right) \tag{3}$$

where H is the relative humidity, and a (kg s^{-1}) and b (kg s^{-1} RH%) are constants which may be determined from the intercept and slope of the plot

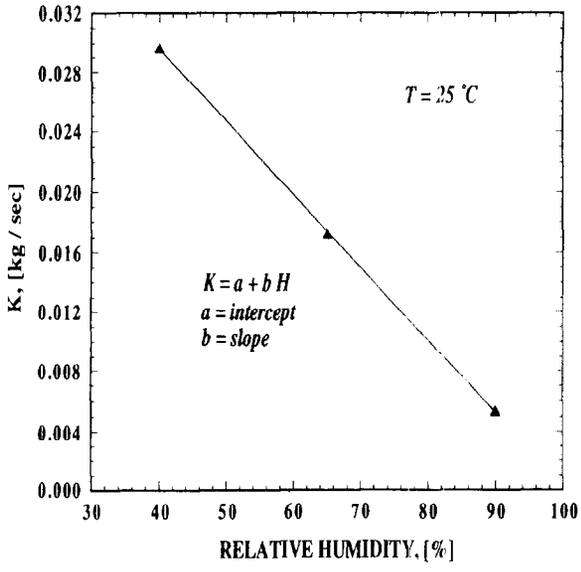

Fig. 14. The constant, K, against the relative humidity for the alumina suspension.

of the constant, K, against the relative humidity which is illustrated in Fig. 14. It should be noted that the values of constants a and b, calculated from Fig. 14, are not normalised with respect to the surface area of the samples. Therefore, they are only valid for that specific surface area and the value of A in eqn (3) should be taken as unity. The drying rates of the suspensions were calculated using eqn (3) with the appropriate values of the parameters (a, b, H, E, T) and compared with the experimental drying rates (Fig. 15). As may be seen from Fig. 15, a good agreement between the predicted and experimental drying rates is observed. After normalising the constants a and b using the information in Section 3.4 and integrating eqn (3), the following equation, which predicts the weight loss of the suspensions as a function of temperature, relative humidity, surface area, and time, is obtained:

$$W = A(a_n + b_n H)\exp\left(-\frac{E}{RT}\right)t \tag{4}$$

where W (kg) is the weight loss, a_n (kg $m^{-2}s^{-1}$) and b_n (kg m^{-2}s RH%) are the normalised constants, and t (s) is time. Equation (4) with the calculated values of the constants (a_n = 389.8 kg m^{-2} s^{-1}, b_n = 3.94 kg m^2 s^{-1} RH%, and E = 41.2 kJ mol^{-1}) will be used to predict the weight loss of the alumina suspensions during the initial stage of drying process.

In order to predict the behaviour during the second stage of the drying, the following equation, which is a solution of the Fick's law diffusion equation, was adopted.[1,9]

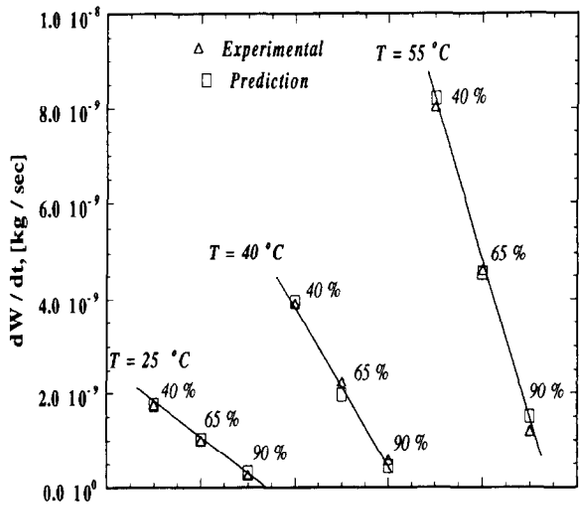

Fig. 15. The predicted and experimental drying rates of the alumina suspensions.

$$W = W_0\left(\exp\left(-Dt(\pi/2d)^2\right) + \frac{1}{9\exp\left(-Dt(\pi/2d)^2\right)} + \frac{1}{25\exp\left(-25Dt(\pi/2d)^2\right)} + \ldots\right) \tag{5}$$

where W is the weight loss, W_o is the initial weight, D is the effective diffusion coefficient, and d is the thickness of the sample. This solution is suitable for the description of the second stage of the suspension drying process since it is formulated for the case of an initially uniform solvent distribution and evaporation from one surface of a slab. It is assumed that the value of D is not a function of the water concentration; this appears to be the case.

It is evident from eqn (5) that the magnitude of effective diffusion coefficient of the water through the matrix will strongly affect the drying kinetics during the second stage. The temperature dependence of the diffusion coefficient, which is conventionally an Arrhenius type of relationship, is given as follows:[1]

$$D = D_o\exp\left(-\frac{E_d}{RT}\right) \tag{6}$$

where D_o is the proportionality constant which is independent of temperature and E_d is the activation energy for the diffusion-controlled stage of drying. In order to calculate the activation energy for the diffusion-controlled stage of suspension drying, the diffusion coefficients at 25, 40, 55, and 70°C were estimated by selecting a suitable value for the diffusion coefficients so that a good agreement between the predicted (using eqn (5)) and the experimental results was obtained. The resulting Arrhenius plot for the diffusion-controlled stage of drying is illustrated in Fig. 16. From the slope of the Arrhenius plot, the activation energy for the diffusion-controlled stage of drying was estimated as *ca.* 37 kJ mol^{-1} which is slightly less than the value observed for the first evaporation stage (see earlier).

The drying curves of the alumina suspensions may then be predicted using eqn (4) for the initial stage of drying and eqn (5) for the diffusion-controlled stage of drying with the appropriate values of the parameters. The predicted and experimental drying curves for the alumina suspensions at various temperatures and sample thicknesses are shown in Figs 17 and 18, respectively. A very good agreement between the predicted and experimental results is observed.

It will be realised that the relationships describing the first (linear) and the second (falling rate)

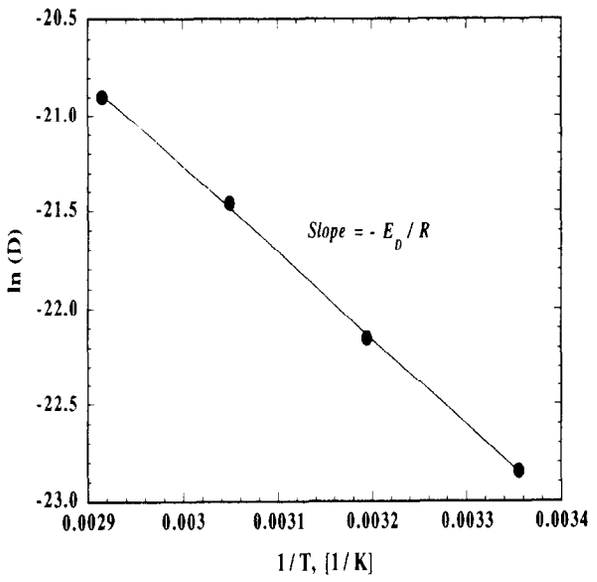

Fig. 16. The Arrhenius plot (ln (D) against ($1/T$)) for the diffusion-controlled stage of drying.

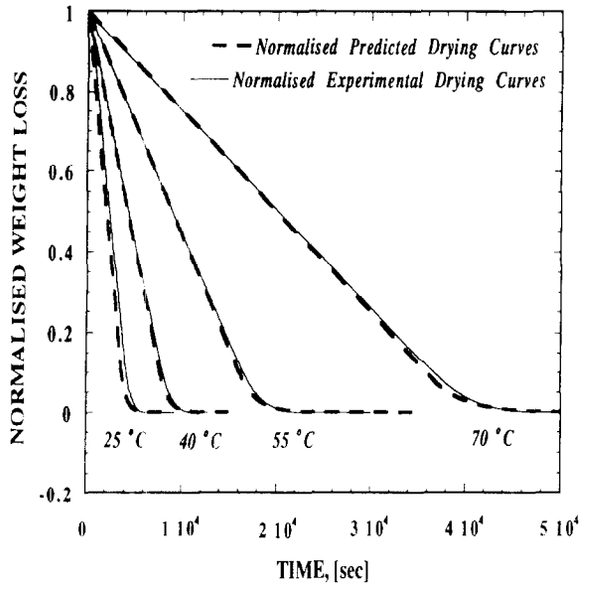

Fig. 17. The predicted and experimental drying curves of the alumina suspensions at 25, 40, 55 and 70°C and the relative humidity of 40%.

stages of the drying process may be used to predict the solvent (water) content over almost the entire drying process providing that a value for the critical point may be selected with reasonable precision. If a value of the water content at the transition (critical) point is chosen as 10% of the initial water content, a satisfactory agreement between prediction and experiments is obtained.

4 DISCUSSION

From the experimental and predicted results, it is clear that the drying of the ceramic suspensions

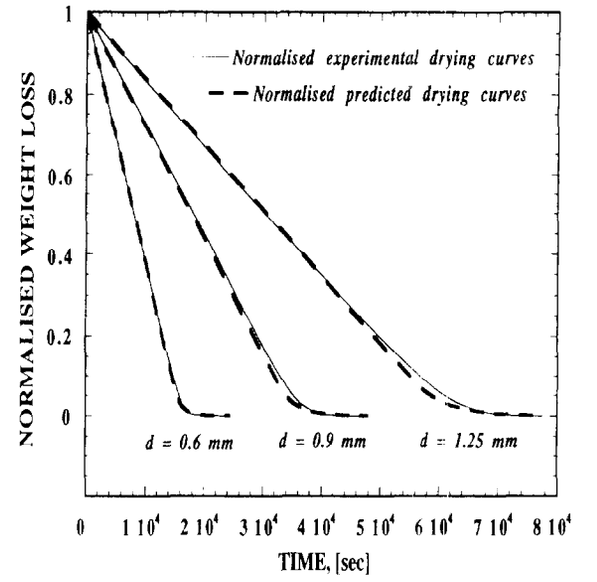

Fig. 18. The predicted and experimental drying curves of the alumina suspensions with the thicknesses of 0.6, 0.9 and 1.25 mm.

involves at least a two stage mechanism. Generally during the drying of the suspensions the following cases may occur:[12]

- Evaporation at the solid surface; resistance to internal diffusion of liquid small as compared with the resistance to the removal of vapour from the surface.
- Evaporation at the solid interface; resistance to internal diffusion of liquid great as compared with the total resistance to the removal of vapour from the surface.
- Evaporation in the interior of the solid; resistance to internal diffusion of the liquid great as compared with the total resistance to removal of vapour.

The drying process will involve one or combinations of these cases. Whatever the mechanism, the drying process of the suspensions takes place in three consecutive steps:[9] mass (liquid or vapour) transportation to the surface, evaporation at the surface, and transportation of vapour from the surface into the ambient gas. The overall rate of the drying process will be determined by the slowest step. The drying of the current ceramic suspensions, in the initial stage, is an example of the case (i) and that where the process is similar to the evaporation of a liquid from a liquid surface. During the initial stage, the overall rate of the drying process is controlled by the interfacial evaporation process at the surface since this step is the slowest step. During the initial stage of the drying of these ceramic suspensions the rate of drying remains remarkably constant. However, as the liquid content of the suspensions decreases the drying

mechanism changes to one of the other three cases, and the rate of drying decreases (falling rate[9]) as the drying process proceeds. Therefore, the drying process of the suspensions is often divided into the constant rate and falling-rate periods. In the falling rate period (in this case the second stage of the suspension drying) the drying kinetics is controlled by the mass (liquid and/or vapour) transportation to the solid surface. At the second stage, the rate controlling drying mechanism is that of the diffusion of water through the solid to the solid surface, where the evaporation takes place, followed by diffusion of the vapour into the air. A more or less stagnant film on the solid surface presents a resistance to the passage of vapour from the solid surface into the ambient air. The sum of this surface resistance to vapour diffusion and the internal resistance to water diffusion through the solid together constitutes the overall resistance to the transfer of water from the interior of the solid to the air. The surface resistance is now negligible compared with the interior resistance to water diffusion. Therefore, the notion of an internal diffusion process may be reasonably used to describe the drying process at the second stage of drying of these ceramic suspensions. We may consider two generic types of internal water transport mechanisms; one based upon capillary flow (viscous) and one arising from vapour transport. We note that the activation energy for the second stage is close to the enthalpy of vaporisation and significantly greater than the 'activation energy' for the viscosity of water; this value is close to 15 kJ mol^{-1}.[13] This would suggest that the internal diffusion is controlled by vapour transport and not capillary flow; the temperature dependence of the surface tension of water is small.

Thus, the initial drying process of the ceramic suspensions is largely controlled by the external, interface phase; an interfacial evaporation process, until the critical point and where *ca.* 90 wt% of the water in the alumina suspensions with *ca.* 40 vol. solid content is removed during this stage. In the final stage the process is also apparently vapour pressure controlled and internal evaporation occurs to facilitate the transport. During the initial stage, as the water is removed, the thickness of the suspensions is greatly reduced. The shrinkage of the thickness of the suspensions is proportional to the weight loss during the initial stage.

5 CONCLUSIONS

The effects of the temperature, the humidity, the surface area, and the sample thickness on the drying kinetics of certain water-based alumina suspensions were investigated using specially constructed apparatus. It has been shown that the drying of the alumina suspensions involves at least a two-stage process; that is, the initial stage of drying is an interfacial evaporation-controlled process and the second stage of drying is a bulk vapour diffusion-controlled process. It has been observed that the drying mechanisms of the alumina suspensions changes from the interface phase evaporation-controlled to the internal diffusion-controlled process at the critical point where *ca.* 90 wt % of the water in the suspension is lost indicating that the majority of the drying process of the alumina suspensions is largely controlled by the interfacial evaporation process. The activation energy for the evaporation process of the alumina suspension was calculated as 42 ± 2 kJ mol^{-1} a value which is also similar to the activation energy values for the water and the water-binder mixture. The activation energy for the diffusion-controlled stage of drying was estimated as 37 ± 2 kJ mol^{-1}; this relatively high value suggests that the bulk migration process is controlled by vapour transport and not capillary flow. The drying curves of the alumina suspensions were predicted very accurately using the equations developed for the evaporation-controlled and diffusion-controlled processes.

ACKNOWLEDGEMENT

This project was supported by the European Human Capital Mobility Programme.

REFERENCES

1. MISTLER, R. E., SHANEFIELD, D. J. & RUNK, R. B., Tape casting of ceramics. In *Ceramic Processing Before Firing*, ed. G. Y. Onoda and L. L. Hench. John Wiley & Sons, New York, 1978 pp. 411–448.
2. WILLIAMS, J., Doctor-blade process. In *Treatise on Materials Science and Technology, Vol. 9, Ceramic Fabrication Processes*, ed. F. F. Wang. Academic Press, New York, 1976 pp. 173–198.
3. MORENO, R., The role of slip additives in tape casting technology: Part I—Solvents and dispersants. *Am. Ceram. Soc. Bull.*, **69**(6) (1990) 1022–1026.
4. MORENO, R., The role of slip additives in tape casting technology: Part II—Binders and plasticizers. *Am. Ceram. Soc. Bull.*, **69**(6) (1990) 1022–1026.
5. HOTZA, D. & GREIL, P., Review: aqueous tape casting of ceramic powders. *Mater. Sci. & Eng.*, **A202** (1995) 206–217.
6. RYU, B. H., TAKAHASHI, M. & SUZIKI, S., Rheological characteristics of aqueous alumina slurry for tape casting. *J. Ceram. Soc. Jpn*, **101**(6) (1993) 643–648.

7. NAGATA, K., Dynamic viscoelastic measurements of suspension for the drying process in tape casting. *J. Ceram. Soc. Jpn*, **101**(8) (1993) 845–849.
8. USHIFUSA, N. & CIMA, M., Aqueous processing of mullite—containing greensheets. *J. Am. Ceram. Soc.*, **75**(9) (1992) 2373–2378.
9. SHERWOOD, T. K., The drying of solids I. *Ind. Eng. Chem.*, **21**(1) (1929) 12–16.
10. DAVIES, J. T. & RIDEAL, E. K. *Interfacial Phenomena*. Academic Press, New York, 1961, p. 5.
11. *Handbook of Chemistry and Physics*. **E–21**, CRC Press, Cleveland, OH, 1997.
12. SHERWOOD, T. K., The drying of solids II. *Ind. Eng. Chem.*, **21**(10) (1929) 976–980.
13. YOSHIMURA, Y., SAWARUMA, S. & TANIGUCHI, Y., Effects of pressure, temperature, and concentration, on the viscosity of aqueous ammonium bromide solutions. *Z. Naturforsch.* **50 a** (1995) 316–322.